Title: Slow-Light and Sensing Performance Analysis on Graphene Metasurface in Terahertz Range Based on Plasmon-Induced Transparency.

Abstract

A simple graphene-based sensing and slow light metamaterial is proposed to demonstrate the dual Plasmon Induced Transparency (PIT) phenomenon that can modulated by varying Fermi Energy, carrier mobility of graphene, and different environmental conditions. The proposed structure is designed for working in the Terahertz range. The PIT phenomena occurred due to destructive interference between two bright and one dark modes. The phenomenon is generated due to strong field and dispersion generated by surface plasmon. The numerical results are produced by employing the FDTD (Finite Difference Time Domain) method. Our proposed structure exhibits a strong sensing capability of 2.1024THz/RIU and a figure of merit (FOM) of 9.01495 which is comparatively stronger than some similar works. It also demonstrates slow light properties and possesses a broad group index of 547. We also calculated the theoretical results of the proposed structure with Coupled Mode Theory (CMT) and it agrees with the simulation result. The optical performance of the proposed design is supposed to contribute to future micro-nano optics

Introduction

Electromagnetically induced transparency (EIT) is a quantum phenomenon that is the result of destructive interference between two dressed states [1] dispersion of EIT is known for significantly slowing the velocity of the light pulses in a medium and thus this feature of EIT can be utilized in different slow light applications. Moreover, it also showed a wide range of great potential in sensing applications [2] However, despite many promising aspects the main problem of EIT is that it often requires extreme experimental conditions that are difficult to maintain. To ease this, we use an analogous concept called PIT (Plasmon Induced Transparency). PIT utilizes surface plasmon polaritons. Surface plasmons are collective oscillations of electrons at the interface between a metal and a dielectric substance, which commonly occurs when a thin metal layer comes into contact with a dielectric medium. In plasmon induced transparency effect the transparency in an opaque region is generated due the coupling between surface plasmon polariton (SPP) mode and planar waveguide mode [3], [4], [5]. In recent years the PIT effect has been achieved in different kinds of metamaterials and metasurface [6], [7], [8], [9], [10]. Graphene, a newly discovered two-dimensional material has depicted many outstanding properties such as optical transparency, extremely fast electron movement, very low ohmic resistance, notably high electron mobility at normal room temperature [11], [12], [13]. More extensive research revealed that graphene also has metal-like properties. It exhibits metalloid

characteristics if the imaginary part of the surface conductivity of graphene is positive, and the real part of the equivalent permittivity is negative. Besides, the real part of complex surface conductivity affects the imaginary part of equivalent dielectric constant of graphene. This results in propagation loss [14]. Graphene also shows resonance in the terahertz band which attracts attention of the researchers [15]

Researchers have demonstrated PIT structures for various applications. For example, PIT sensor which is a surface plasmonic sensor uses surface plasmon resonance principles to detect changes in the refractive index of a substance near the sensor's surface [16]. But at first metal-based PIT sensors were being used. The inherent high-level ohmic losses in metals provide one of the main difficulties with SPs. As a result, SPs decay quickly, limiting their propagation distance and preventing them from achieving high transmittance and Q factor. It has recently been shown that the high-refractive index dielectric metasurface-based PIT offers an alternate technique to overcome the enormous nonradiative losses in metal because ohmic non radiative losses in the dielectric are less significant. Again, electrons could tunnel through insulating dielectric layers, resulting in non-radiative losses. Polarization effects are the main cause of this loss mechanism on dielectric surfaces. However, our study uses graphene as a dielectric material for PIT ordered by an atomic-scale hexagonal lattice made of carbon atoms. As far as we know, the fermi level in graphene can be changed dynamically by applying chemical doping, electrostatic gating or magnetic field. Therefore, it is possible to create firmly adjusted PIT systems by combining graphene with metasurface. Furthermore, the metasurface, being a distinct structural type, holds significant potential for use in integrated optoelectronic devices and planar sensors. Likewise, adjusting the geometrical parameters of the metasurface structure may allow for tuning an all-dielectric PIT resonance to a desired electromagnetic wavelength. Again, the transmission spectrum is continuously evolving to provide sensors with acceptable characteristics because of the huge waist caused by the ohmic loss of meta used in SPs in the optical regime. Take into consideration a PIT that consists of both bright and dark settings and has a small transparency window to solve this problem. Plasmon-induced transparency (PIT) is a phenomenon that happens when two or more plasmonic resonances interact, resulting in a narrow transparency window inside the border spectrum [17] Because of its broad prospective applications in chip (on/off) nanodevices such as slow light devices [18]. Plasmon-induced transparency can also be used in a variety of applications, particularly sensing and detection [[19] PIT based sensors have been proposed for a variety of wavelength ranges, including visible [20], [21], [22], [23], However, plasmonic devices which are made of noble materials have significant limitations, such as SPR propagation in metal cavities with considerable attenuation. Graphene, which is made-up of a single sheet of carbon atoms, has gained popularity in recent years due to its two-

dimensionality and several benefits over noble metals [24]. Graphene works best in the terahertz range; we use this range for our structure [25]

Though graphene-based metamaterial has been used for quite a time now, there are only a few multifunctional structures that can be used for more than one purpose at the same time. In our paper we are proposing a novel single layer graphene meta surface structure that shows both excellent sensing and slow light properties. The graphene layer is placed on the top of the substrate. The Si structure is a dielectric substrate and the graphene metasurface acts like a metal for generating SPPs. Thus, our structure utilizes the PIT phenomenon. The PIT response can be tuned with the help of Fermi energy, E_f of the graphene layer. The Fermi energy, Ef is controlled by external voltage. Besides, CMT (Coupled Mode Theory) is employed to calculate the transmission, reflection and absorption theoretically [26]. Almost similar result from both FDTD simulation and CMT verifies the response our design. Our design shows greater sensitivity and_ FOM as a sensor and excellent slow light property of the group index. Thus, our paper analyzes the optical response of our proposed structure in terms of PIT to show sensing performance and slow light applications.

Structural design and Analysis:

The three-dimensional structure of the proposed PIT based tunable graphene-silicon sensing and slow light metamaterial is shown in Fig.1(a). A single layer of graphene pattern is deposited on the top of the Si substrate. A bias circuit was established to connect doped Si and graphene and to tune the graphene fermi energy with voltage. The thickness of Si substrate is 0.1 μm. The relative permittivity of silicone is 11.9 [27] . The graphene layer is a two-dimensional layer. The structure is periodic in both the x axis and y axis. A plane wave source is from the positive direction of the z axis as an excitation source. For this paper, we opted for the FDTD (Time Domain Finite Difference) method for the numerical simulation result. We used periodic boundaries both in x direction and y direction while using PML (Perfectly Matched Layer) in z direction.

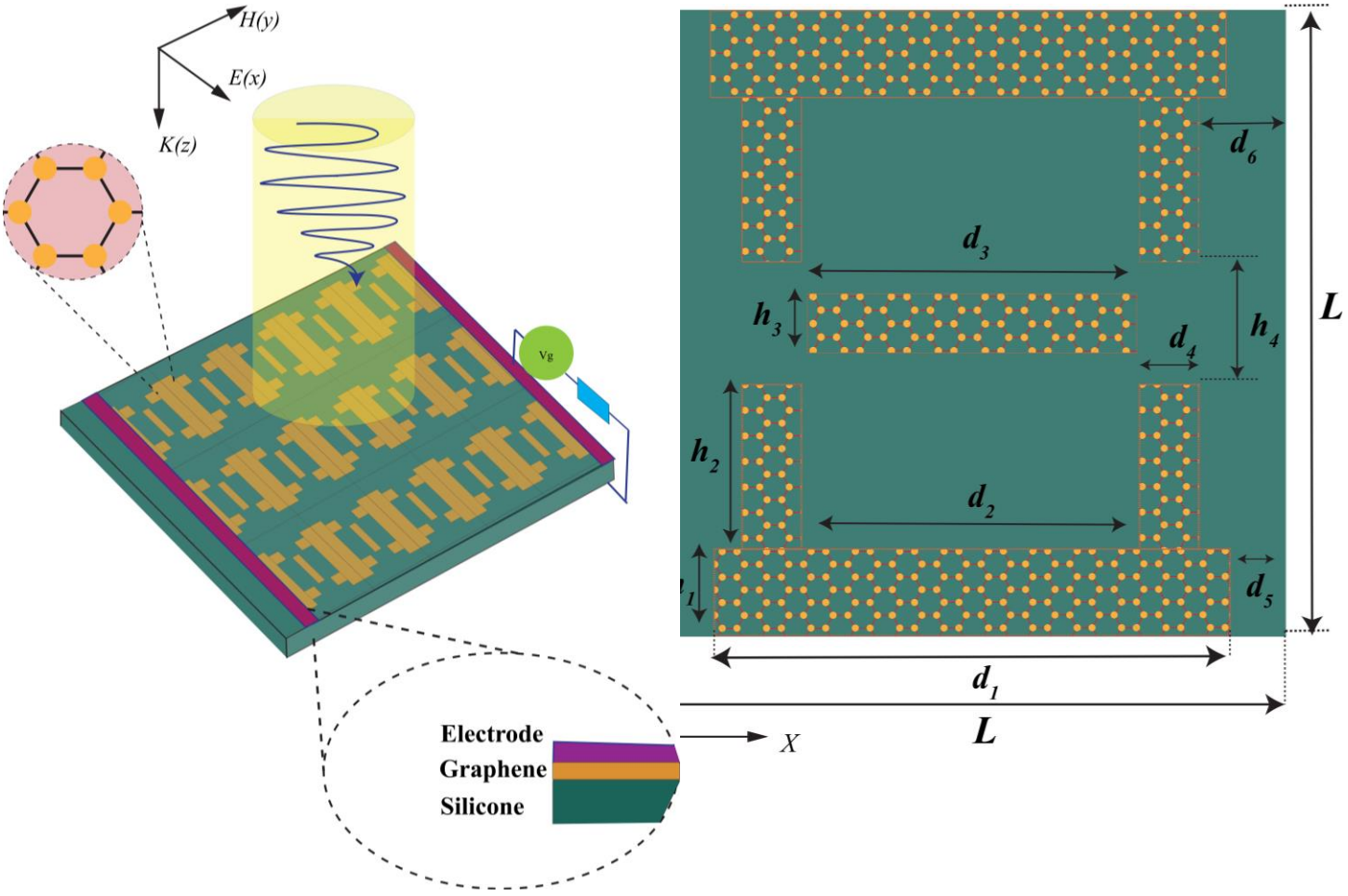

(a) (b)

Fig.1: (a) Lateral view of graphene-based dual PIT slow-light and sensing structure. **(b)**Top view of the sensor structure. The thickness of the silicon layer is 0.1 μm, respectively. Geometric criteria of the unit cell: L = 5.0 μm, d_1 = 3.0 μm, d_2 = d_3 = 1.6 μm, d_4 = 0.5 μm, d_5 = 1.0μm, d_6 =1.2 μm. h_1 = 1.1 μm, h_2 = 0.75 μm, h_3 = 0.5 μm, h_4 = 1.3 μm.

The two-dimensional top view of the proposed structure's unit cell is illustrated in Fig.1(b). As we can see, our structure is composed of 3 horizontal & 4 vertical graphene nanoribbons. The unit cell of the proposed pattern is symmetric both in x axis and y axis. The length of the whole unit structure is given by L. Besides, d_1, d_3, d_4 are the length of the graphene nanoribbons and h_1 , h_2, h_3 are the width of these nanoribbon. The E_f could be easily adjusted by tuning the bias voltage between electrode and substrate. Our proposed device performs in the terahertz region. So, the surface conductivity of graphene is given by Drude like model [28], [29]:

$$\sigma = \frac{e^2 E_f}{\pi \hbar^2} \frac{i}{(\omega + i\tau^{-1})} \quad (1)$$

Structure Response:

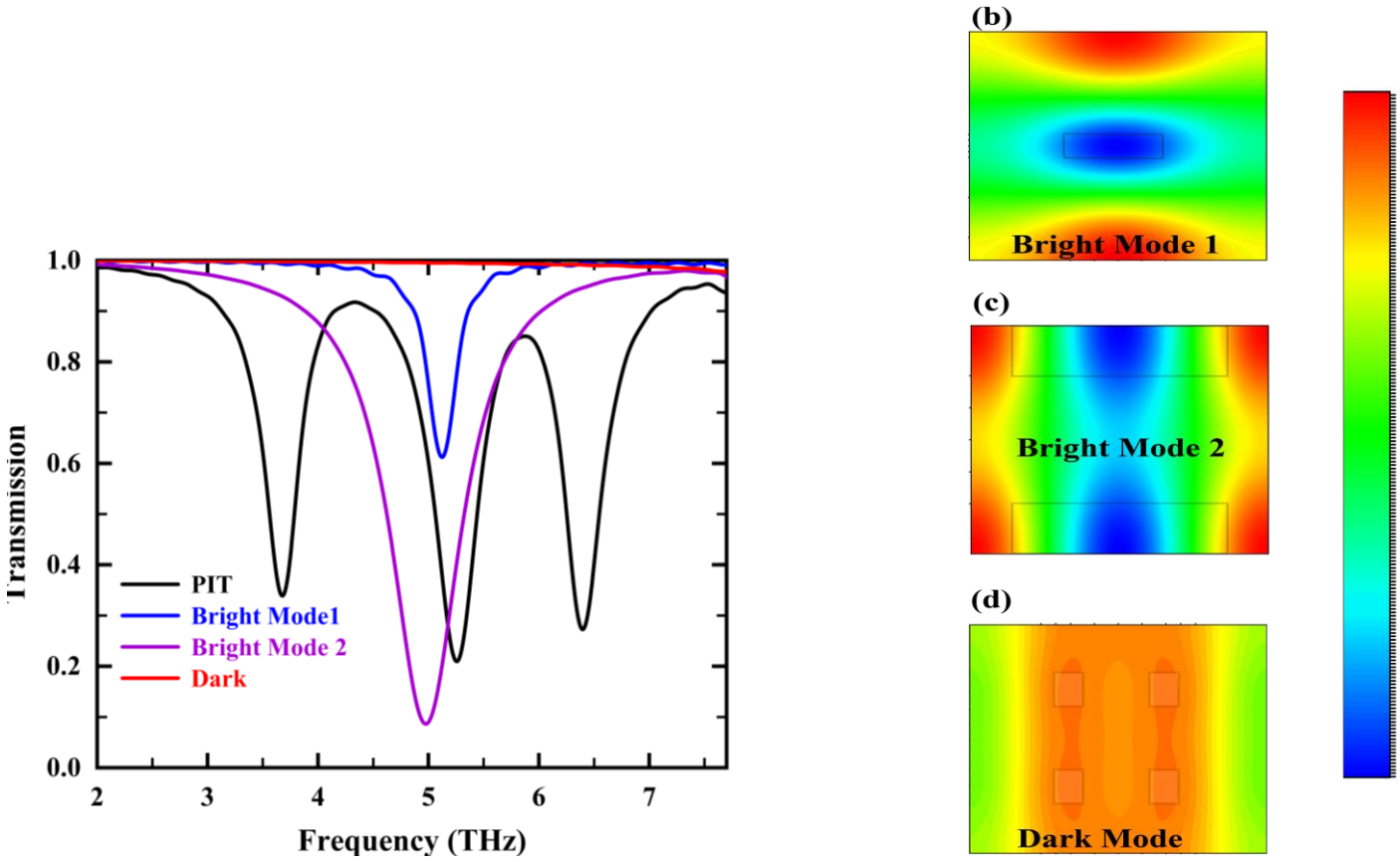

(a)

Fig. 2: (a) The transmission spectrum of the proposed PIT metamaterial at E_f=0.7 eV. The transmission is given in black solid line.TH response of the two bright mode and one dark mode is illustrated in blue, violet and red solid lines respectively. The electric field distribution of the **(b)** Bright mode 1, **(c)**Bright mode 2 and **(d)** Dark mode.

The equation abides by the following condition for simplification: $E_f \gg k_B T$. Here i, e, E_f, k_B, $\hbar$, ω, τ, respectively, are the imaginary unit, elementary charge, Fermi voltage, Boltzmann constant, reduced Planck's constant, angular frequency and carrier relaxation time. The temperature of the whole setup was kept at 300 K. The carrier relaxation time τ is measured with the following

equation:$\tau = \mu E_f/(ev_F^2)$, here, μ and v_F are the carrier mobility and the Fermi velocity, respectively. In our simulation space the μ was kept at 1 $m^2 V^{-1} s^{-1}$and v_F was kept at 10^6 ms^{-1} [30]. The proposed structure has two bright modes and one dark mode. The bright modes can be independently excited by the source, but dark modes aren't. Two side horizontal graphene nanoribbons give rise to the first bright mode and middle nanoribbon gives rise to the second bright mode. The four horizontal graphene beams are responsible for dark modes. So, the four horizontal graphene nano strips can't be excited on their own. But when coupled with other two bright modes they are also excited and thus the third dip is generated. It gives rise to dual PIT phenomenon. From various simulation data, the E_f of the bright modes were set to be 0.7 eV and the bias voltage of dark mode was adjusted in the range of 0.5 eV to 0.9 eV in the electrode. To further investigate the dual PIT phenomenon, we utilize the coupled mode theory or CMT [31], [32] to break down the mechanism of coupling between two bright modes and one dark mode of our proposed graphene structure theoretically. The theoretical model of CMT is described in Fig. 2. We use A, B and C for describing three modes. We denote the amplitudes of three modes as a, b and c respectively. $A_{\pm}^{in/out}$, , $B_{\pm}^{in/out}$ and $C_{\pm}^{in/out}$ represent input or output waves propagating in the opposite or positive direction of the hypothetical resonator. The superscript "in" represents the input waves and "out," represents the output waves in these imaginary resonators. The subscript "+" stands for positive direction and "-" stands for the negative directions along the resonators. We use μ_{nm} for denoting the coupling co-efficient among these three couplers (n, m =1, 2, 3, n ≠ m). The internal and external loss components of these three resonators are denoted by γ_{in} and γ_{out} respectively. To further investigate the dual PIT phenomenon, we utilize the coupled mode theory or CMT [31], [32] to break down the mechanism of coupling between two bright modes and one dark mode of our proposed graphene structure theoretically. The theoretical model of CMT is described in Fig. 2. We use A, B and C for describing three modes. We denote the amplitudes of three modes as a, b and c respectively and represent input or output waves propagating in the opposite or positive direction of the hypothetical resonator. The superscript "in" represents the input waves and "out," represents the output waves in these imaginary resonators. The subscript "+" stands for positive direction and "-" stands for the negative directions along the resonators. We use for denoting the coupling co-efficient among these three couplers (n, m =1, 2, 3, n ≠ m). The internal and external loss components of these three resonators are denoted by and respectively.

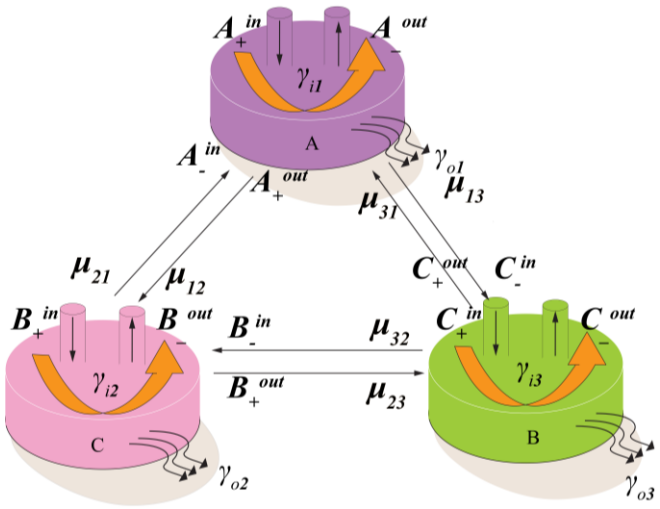

Fig 3.: Schematic diagram of coupled mode theory(CMT).

Here, $\gamma_n = i\omega - i\omega_n - \gamma_{in} - \gamma_o$ and $\gamma_{in} = \omega_n / 2Q_{in}$. Here, Q_{in} and Q_{on} denote the internal loss quality factor and the external loss quality factor, respectively. We also can mention that:

$$\frac{1}{Q_{tn}} = \frac{1}{Q_{in}} + \frac{1}{Q_{on}} \tag{2}$$

Here, Q_{tn} is the total quality factor of the n th hypothetical resonator. The total quality factors Q_{tn} can be calculated by the formula, $Q_{tn} = f_n/\Delta f_n$. Here f_n is resonating frequency of the n the mode, Δf_n is the FWHM of the resonating frequency. The internal loss quality factor can be determined by

$$Q_{in} = Re(neff_n)/Im(neff_n) \tag{3}$$

Here, $neff = \beta/k_0$ is the effective refractive index. β is the propagation constant. $k_0 = \omega/c$ is the wave vector [33]

$$\beta = k_0 \sqrt{\varepsilon - \left(\frac{2\varepsilon}{\eta_0 \sigma}\right)^2} \tag{4}$$

When the light is incident t on the resonator A, it goes through resonator B and finally it comes out from the final resonator C. The relationships between these three couplers can be given by:

$$B_+^{in} = A_+^{out} e^{i\varphi_1} \quad , A_-^{in} = B_-^{out} e^{i\varphi_1} \tag{5}$$

$$C_+^{in} = B_+^{out} e^{i\varphi_2} \quad , B_-^{in} = C_-^{out} e^{i\varphi_2} \tag{6}$$

$$A_+^{out} = A_+^{in} - \gamma_{o1}^{1/2} a \quad , A_-^{out} = A_-^{in} - \gamma_{o1}^{1/2} a \tag{7}$$

$$B_+^{out} = B_+^{in} - \gamma_{o2}^{1/2} b \quad , B_-^{out} = B_-^{in} - \gamma_{o2}^{1/2} b \tag{8}$$

$$C_+^{out} = C_+^{in} - \gamma_{o3}^{1/2} c \quad , C_-^{out} = C_-^{in} - \gamma_{o3}^{1/2} c \tag{9}$$

$$C_-^{in} = 0 \tag{10}$$

Here, φ_1 is the phase difference between Mode A and Mode B respectively,φ_2 is the phase difference between mode B and Mode C. But as these three hypothetical resonators reside on the same plane there is no phase difference between them if the light is perpendicularly incident on them. So, $\varphi_1 = \varphi_2 = 0$. So, the transmission co-efficient of the spectrum can be written as:

$$t = \frac{C_+^{out}}{A_+^{in}} = 1 - \gamma_{o1}^{1/2} D_1 - \gamma_{o2}^{1/2} D_2 - \gamma_{o3}^{1/2} D_3 \tag{11}$$

The reflection co-efficient of the spectra can be written as:

$$r = -\gamma_{o1}^{1/2} D_1 - \gamma_{o2}^{1/2} D_2 - \gamma_{o3}^{1/2} D_3 \tag{12}$$

The co-efficient in the equation (11) and (12) can be represented by the following equations.

$$D_1 = \frac{(\gamma_2\gamma_3 - \gamma_{23}\gamma_{32})\gamma_{o1}^{1/2} + (\gamma_{12}\gamma_3 + \gamma_{13}\gamma_{32})\gamma_{o2}^{1/2} + (\gamma_{12}\gamma_{23} + \gamma_{13}\gamma_2)\gamma_{o3}^{1/2}}{\gamma_1\gamma_{23}\gamma_{32} - \gamma_1\gamma_2\gamma_3 + \gamma_{12}\gamma_{21}\gamma_3 + \gamma_{12}\gamma_{23}\gamma_{31} + \gamma_{13}\gamma_{21}\gamma_{32} + \gamma_{13}\gamma_2\gamma_{31}} \tag{13}$$

$$D_2 = \frac{(\gamma_{21}\gamma_{33} + \gamma_{23}\gamma_{31})\gamma_{o1}^{1/2} + (\gamma_1\gamma_3 - \gamma_{13}\gamma_{31})\gamma_{o2}^{1/2}\gamma_{1+} (\gamma_{23}\gamma_{13} + \gamma_{13}\gamma_{21})\gamma_{o3}^{1/2}}{\gamma_1\gamma_{23}\gamma_{32} - \gamma_1\gamma_2\gamma_3 + \gamma_{12}\gamma_{21}\gamma_3 + \gamma_{12}\gamma_{23}\gamma_{31} + \gamma_{13}\gamma_{21}\gamma_{32} + \gamma_{13}\gamma_2\gamma_{31}} \tag{14}$$

$$D_3 = \frac{(\gamma_{21}\gamma_{32} + \gamma_2\gamma_{31})\gamma_{o1}^{1/2} + (\gamma_1\gamma_{32} + \gamma_{12}\gamma_{31})\gamma_{o2}^{1/2} + (\gamma_1\gamma_2 - \gamma_{12}\gamma_{21})\gamma_{o3}^{1/2}}{\gamma_1\gamma_{23}\gamma_{32} - \gamma_1\gamma_2\gamma_3 + \gamma_{12}\gamma_{21}\gamma_3 + \gamma_{12}\gamma_{23}\gamma_{31} + \gamma_{13}\gamma_{21}\gamma_{32} + \gamma_{13}\gamma_2\gamma_{31}} \tag{15}$$

$$\gamma_{12} = i\mu_{12} + (\gamma_{o1}\gamma_{o2})^{1/2} \quad , \gamma_{13} = i\mu_{13} + (\gamma_{o1}\gamma_{o3})^{1/2} \tag{16}$$

$$\gamma_{21} = i\mu_{21} + (\gamma_{o1}\gamma_{o2})^{1/2} \quad , \gamma_{23} = i\mu_{23} + (\gamma_{o2}\gamma_{o3})^{1/2} \tag{17}$$

$$\gamma_{31} = i\mu_{31} + (\gamma_{o1}\gamma_{o3})^{1/2} \quad , \gamma_{32} = i\mu_{32} + (\gamma_{o2}\gamma_{o3})^{1/2} \tag{18}$$

So, the transmission of the spectra can be determined by, $T = t^2$. Similarly, the reflection of the spectra is obtained from, $R = r^2$. Also, the absorbance of the spectra is, $A = 1 - T - R$.

Structural parameters:

Our proposed graphene-based PIT metamaterial has different transmission spectra if different structural parameters are changed. So, we experimented with different parameters to achieve the optimized result from our structure. If the value of d1 is increased there is a red shift in the Transmission. But decreasing the d1 to less than 3.2 µm .

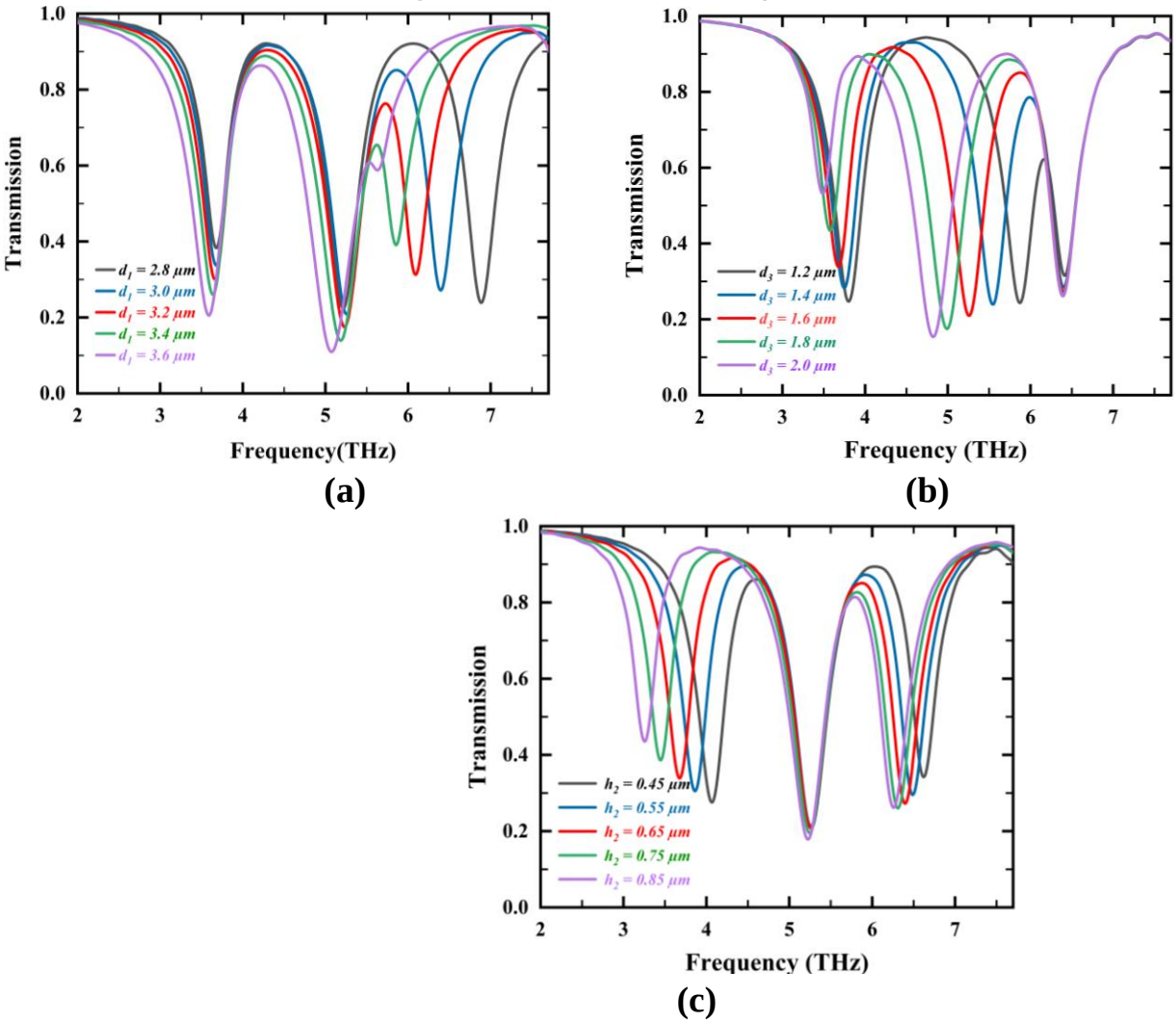

Fig. 4: PIT transmission when (a) d_1,(b) d_2 and (c) h_2 have different dimensions.

results in significant decrement of transmission for dip1 and dip2. Increasing d_3 also produces red shift but the transmission peak of dip 1 greatly reduces. Besides increasing d_3 produces less sensitivity. Moreover, reducing it too much can also produce less sensitivity. Smaller values of h_2 can cause interference of dip 2 with dip1 and dip3 as the spectrum shrinks if the value of h_2 is very small and transmission of dip1 and dip3 is affected if h_2 is large. So, we have opted for d_1 = 3.2 µm, d_3 = 1.6 µm and h_2 = 0.65 µm which are depicted in red solid line in Fig. 4(a-c) respectively. We use these values for an optimized structure.

Fabrication Feasibility:

For possible fabrication of the proposed device uv lithography technique can be applied. UV lithography can be a efficient way to deposit 2D graphene layer on top of a Si substrate. First a thin film Si of 0.1 um is grown in PECVD technique. Then Si is patterned into arrays using photolithography. The proposed pattern of graphene can be used for masking. Afterwards the AgF can be used to fill the channel created.

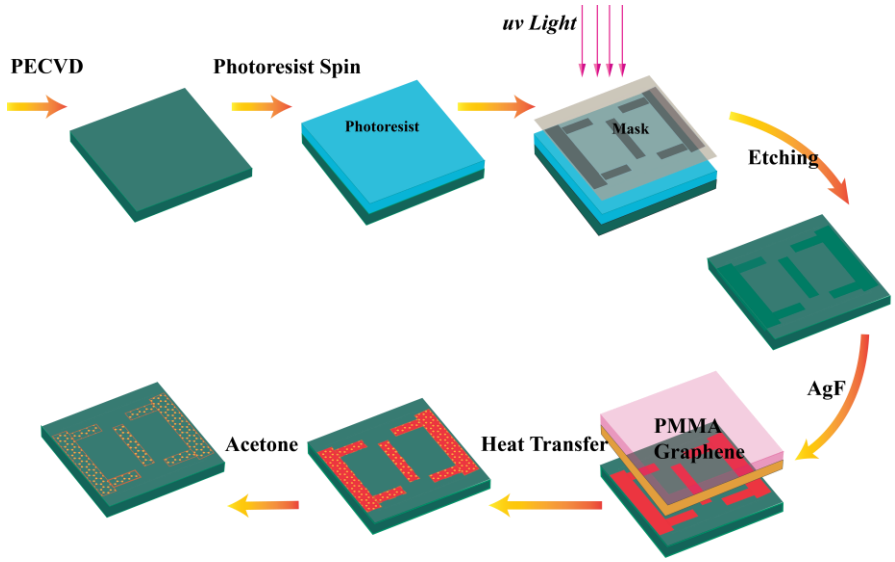

Fig. 5: Fabrication steps of unit cell of the sensor.

Then it needs to be covered with graphene. After that it should be annealed it at 100-degree Celsius temperature. It helps in the efficient fluorination of graphene which only keeps the graphene only in AgF filled areas [34].

Result and Discussion:

The transmission spectra of proposed graphene structure at different Fermi levels were numerically calculated using FDTD and was recorded to observe the relationship between transmission and Fermi energy, E_f. When the E_f was increased from 0.5 eV to 0.9 eV.

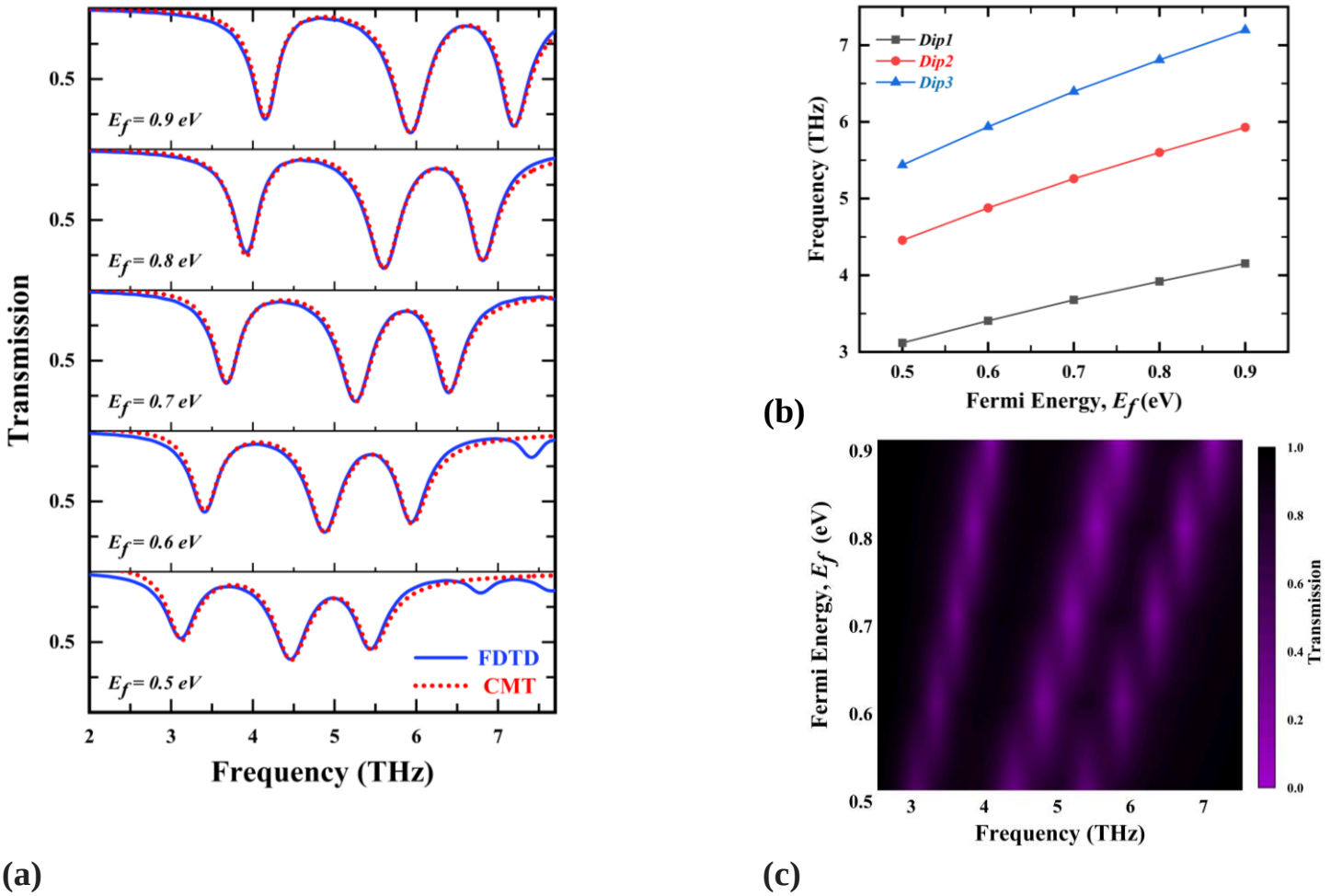

Fig. 6 (a) The transmission spectra of the proposed graphene PIT metamaterial at terahertz band when E_f *is* equal to 0.5eV, 0.6eV, 0.7eV, 0.8eV, 0.9eV from top to bottom. Here, the graphene mobility, μ = 1 m^2/Vs; **(b)**The shift in the frequency of the dip1, dip 2 and dip 3 corresponding with the changing E_f Fig. 3(a); **(c)**The functional relationship between changing E_f, frequency and transmittance by theoretical calculation for the proposed device.

numerical calculation done with FDTD method in blue solid lines. We also calculated the theoretical transmission spectra using CMT and it is included in red dotted line in Fig. 3(a). We can see that CMT results agree with FDTD results excellently. When the E_f was increased from 0.5 eV to 0.9 eV, there is significant blue shift in transmission spectra as illustrated in Fig. 3(b). As we can observe in Fig. 3(b) the transmission of dip1, dip2 and dip3 can reach up to 0.21482, 0.11744 and 0.16556 at the resonating frequency of 4.1535 THz, 5.92881 THz and 7.198 THz if the Fermi level is 0.9 eV. So, the transmission spectra of PIT for the structure can be effectively

tuned with Fermi level. Additionally, Fig.3(c) discusses the functional relationship between Fermi energy and transmission at different frequency in terahertz range.

For further investigation, we also recorded the absorption and reflection spectra at different Fermi energy of the proposed PIT structure in Fig.4.The FDTD simulated spectra is recorded in blue solid lines and the theoretical results are depicted in red dotted lines in Fig. 4(a) we can also notice the blue shift in reflection spectra with the increment in Fermi level. Besides, it is worth mentioning that reflectance peaks increase with increasing Fermi voltage. Fig. 4(b) illustrates the absorption spectra of the proposed structure in different Fermi levels. The three absorption peaks also produce blue shifts. The structure has the highest absorption peak of 0.49817 at 6.38821 THz when E_f is equal to 0.7 eV. So, our proposed structure could be an effective absorber or reflector in terahertz band.

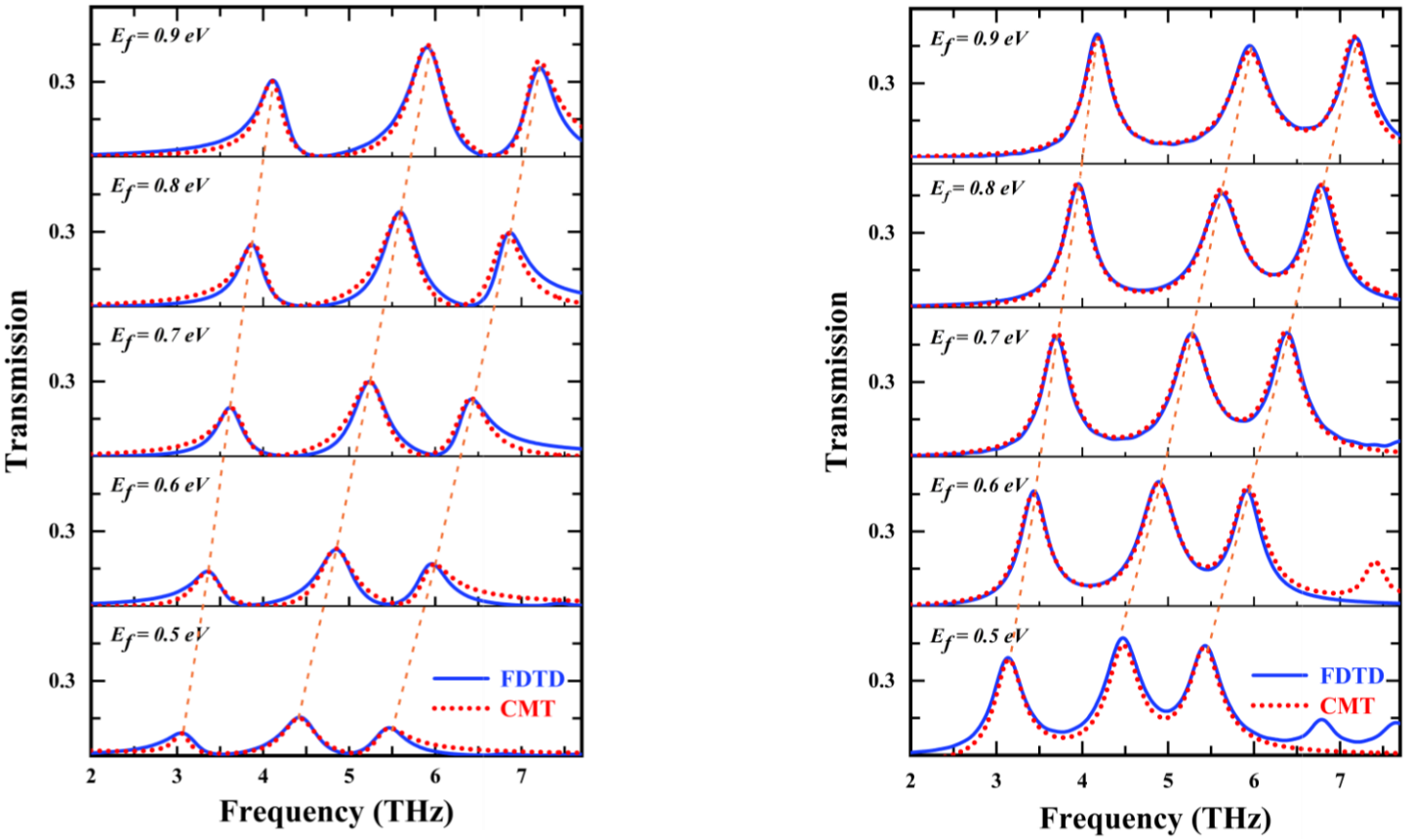

(a) **(b)**

Fig. 4: (a) The reflection **(b)** absorption spectra of the proposed graphene PIT metamaterial at terahertz band when E_f *is* equal to 0.5eV, 0.6eV, 0.7eV, 0.8eV, 0.9eV from top to bottom. Here, the graphene mobility, $\boldsymbol{\mu}$ = 1 m^2/Vs;

The transmission spectra of the proposed structure under different polarization angles are illustrated in Fig. 8. The proposed structure is symmetrical both separately in x axis and y axis. So, the structure works best when polarization angle is 0°. When we increase the polarization angle

the overall response is very distorted and the transmission is lesser with increasing angle till 45°. Although there is no blue or red shift seen till 45°.But after that we see that there is a red shift in the response at 60° although the response is still very distorted.

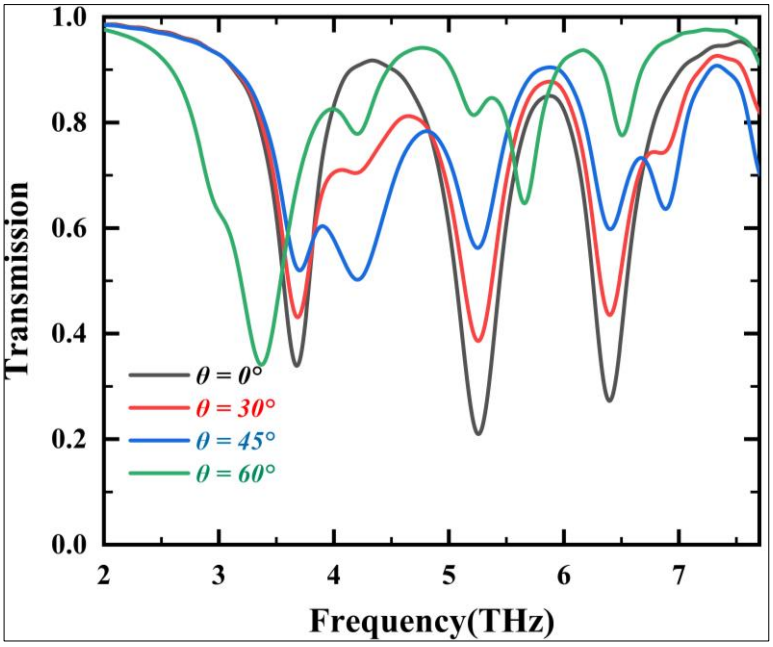

Fig. 8: PIT Transmission at different polarization angle

Slow-Light Performance

Graphene has excellent dispersive property that can be very useful for slowing down the velocity of the photons. Using CMT transmission co-efficient, theoretical and complex phase shift was derived. If the transmission co-efficient is t, then the phase, $\theta = \arg(t)$. The group index can be measured as ,

$$n_g = \frac{c}{v_g} = \frac{c}{t}\frac{d\theta}{d\omega}$$

Here, ***c*** is the velocity of light, $\boldsymbol{v_g}$ is the group velocity and ***t*** is the thickness of silicon substrate. The change of phase shifts and group index at different Fermi levels are depicted in Fig. 9(a-d). As the light is incident on the graphene surface plasmons are generated and they propagate along the interface of graphene and dielectric. But there is no linear relationship between the angular frequency and propagation constant. Near field coupling between bright and dark modes causes strong dispersion resulting in sudden change in phase, consequently resulting in sudden group index change. Our proposed structure shows a maximum group index of 547 at Fermi energy of 0.9 eV which is better than a lot of other proposed structures.

Table I.

	Our Proposed	Ref[35]	Ref [36]	Ref [37]	Ref [38]	Ref [39]
Group Index	547	511	382	328	321	469

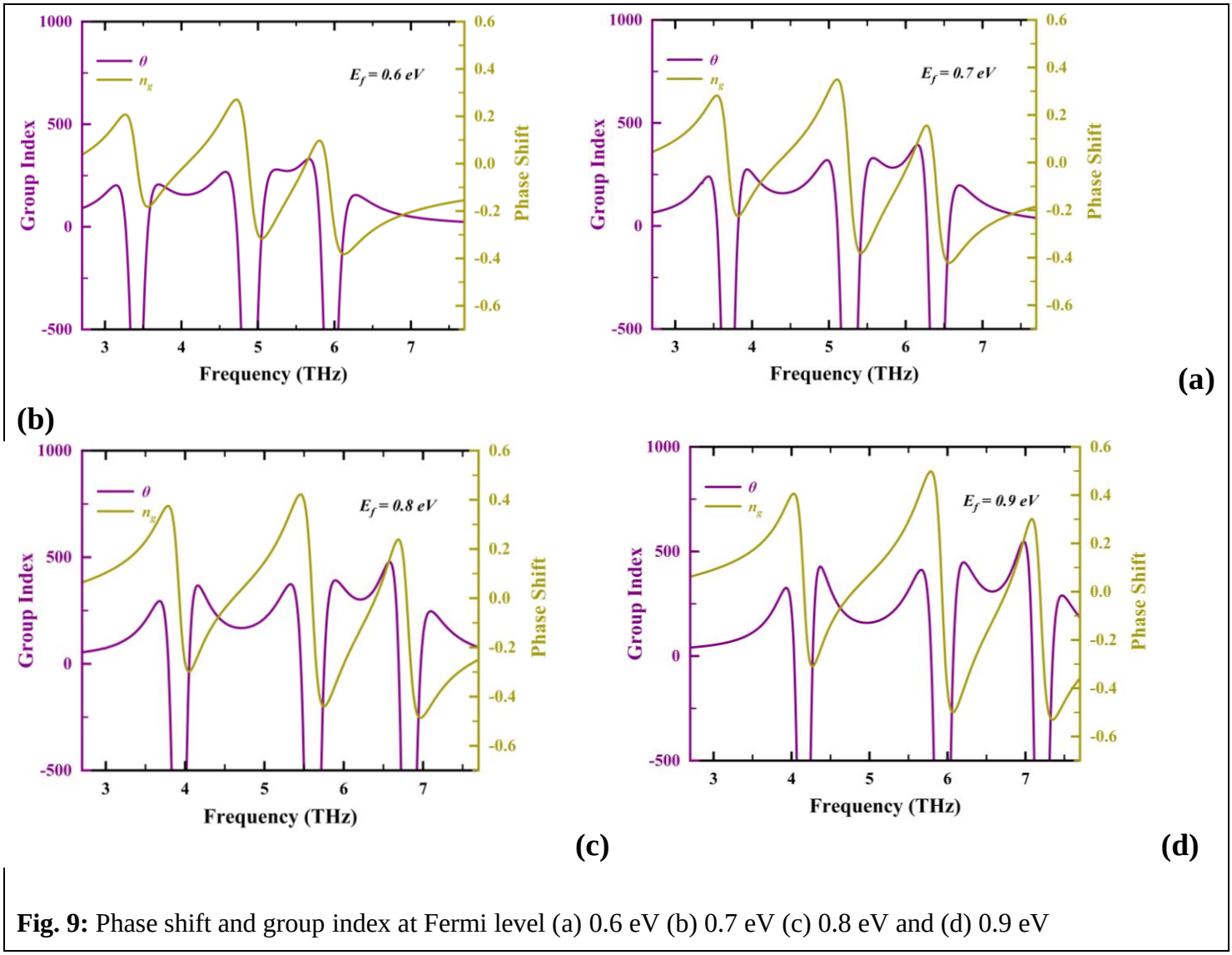

Fig. 9: Phase shift and group index at Fermi level (a) 0.6 eV (b) 0.7 eV (c) 0.8 eV and (d) 0.9 eV

Sensitivity Performance

PIT transmission spectra changes with the change in external refractive index. The resonance frequency of the transmission window sees a shift with changing refractive index. So, our graphene-based PIT metamaterial structure can also be used for sensing operation. The

transmission spectra at different refractive index in depicted in Fig. 9(a). The E_f is kept constant at 0.7 eV and the mobility μ is set to 1 $m^2 V^{-1}$.

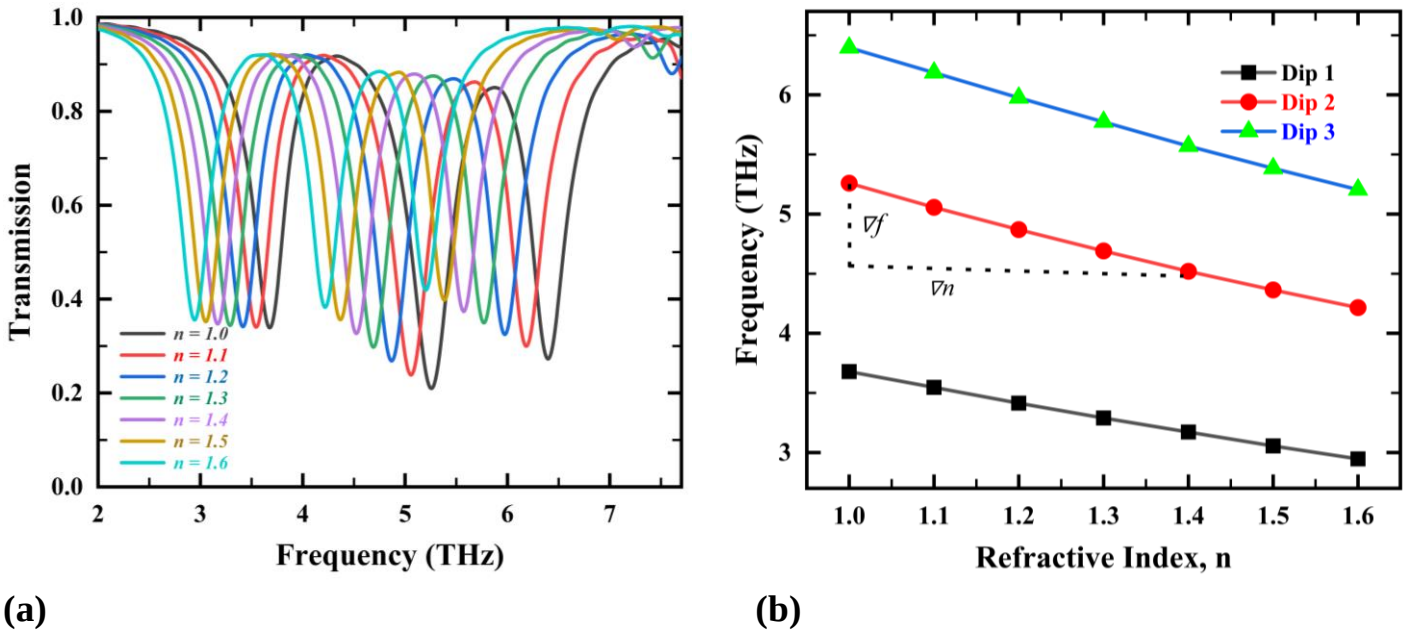

Fig. 10: (a) Transmission spectra of our proposed graphene metasurface as a function of refractive indexes (E_f= 0.7 eV). (b) Functional relationship between frequency, *f* and refractive index, *n*.

There is a clear red shift with an increasing refractive index. So, we have performed a liner fitting for dip1, dip2 and dip3 for different refractive index in Fig. 9(b). It further proofs that our sensor gives a linear redshift which is pretty advantageous for sensing activity. We can determine sensitivity from the slope of these curves in Fig. 9(b). The sensitivity can be determined by, $S = \Delta f / \Delta n$, where ∇f is the difference of resonating frequency and ∇n is the refractive index difference. We have recorded the values of ∇f and ∇n in table II.

Table II.

∇f_1 (THz)	∇f_2 (THz)	∇f_3 (THz)	S_1 (THz/RIU)	S_2 (THz/RIU)	S_3 (THz/RIU)
0.13237	0.20245	0.21024	1.3237	2.0245	2.1024
0.13237	0.18687	0.21023	1.3237	1.8687	2.1023

0.12458	0.17909	0.20245	1.2458	1.7909	2.0245
0.1168	0.1713	0.20245	1.168	1.713	2.0245
0.11679	0.15573	0.18687	1.1679	1.5573	1.8687
0.10901	0.14794	0.17909	1.0901	1.4794	1.7909

Our proposed structure has maximum sensitivity of 1.3237 THz/RIU, 2.0245 THz/RIU and 2.1024 THz /RIU for dip1, dip2 and dip3 which indicates an excellent sensitivity performance.

Figure Of Merit (FOM) Analysis:

Another way of analyzing a sensor's sensing activity is through the Figure of Merit (FOM). It is a method to determine how fast a sensor can react to changes in refractive index. FOM can be determined by, $FOM = \Delta T/T\Delta n$ .. .. Here ΔT is the difference in transmission at different n

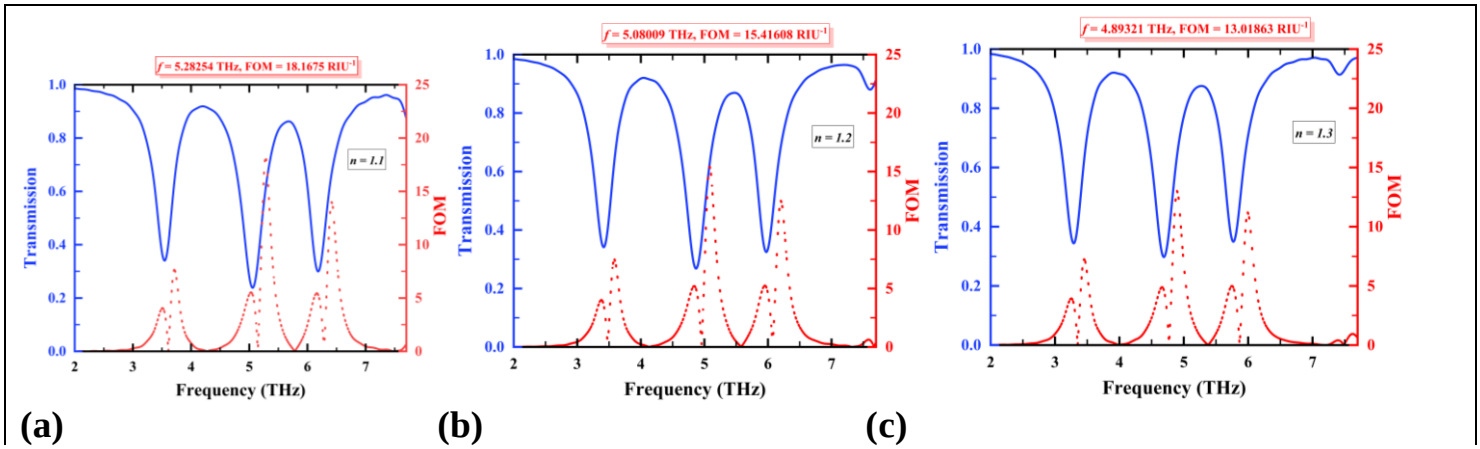

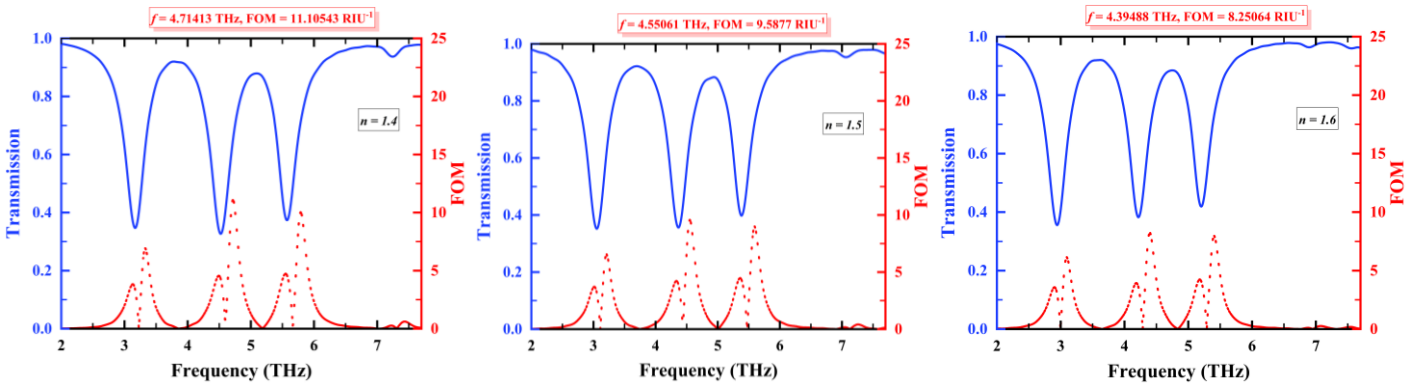

(d) **(e)** **(f)**

Fig. 11: Figure of merit at refractive index **(a)** n = 1.1, **(b)** n = 1.2, **(c)** n = 1.3, **(d)** n = 1.4, **(e)** n = 1.5 and **(f)** n = 1.6.

We get the highest FOM of 18.41 for n=1.1 which is also better than many past proposed sensors. The sensitivity and FOM is compared in table III.

Table III.

	Our Proposed	Ref [35]	Ref [40]	Ref [41]	Ref [42]	Ref [43]
Sensitivity (THz/RIU)	**2.1024**	**.7928**	**1.71314**	**1.7745**	**0.36**	**1.7134**
FOM (RIU^{-1})	**18.41**	**8.12**	**6.998**	**23.61**	**3.64**	**144.45**

[1] K.-J. Boller, A. Imamoğlu, and S. E. Harris, "Observation of electromagnetically induced transparency," *Phys Rev Lett*, vol. 66, no. 20, pp. 2593–2596, May 1991, doi: 10.1103/PhysRevLett.66.2593.

[2] L. V. Hau, S. E. Harris, Z. Dutton, and C. H. Behroozi, "Light speed reduction to 17 metres per second in an ultracold atomic gas," *Nature*, vol. 397, no. 6720, pp. 594–598, Feb. 1999, doi: 10.1038/17561.

[3] A. V. Zayats, I. I. Smolyaninov, and A. A. Maradudin, “Nano-optics of surface plasmon polaritons,” *Phys Rep*, vol. 408, no. 3–4, pp. 131–314, Mar. 2005, doi: 10.1016/j.physrep.2004.11.001.

[4] K. Shastri, M. Abdelrahman, and F. Monticone, “Nonreciprocal and Topological Plasmonics,” *Photonics*, vol. 8, no. 4, p. 133, Apr. 2021, doi: 10.3390/photonics8040133.

[5] S. Farhadi, M. Miri, and A. Farmani, “Plasmon-induced transparency sensor for detection of minuscule refractive index changes in ultra-low index materials,” *Sci Rep*, vol. 11, no. 1, p. 21692, Nov. 2021, doi: 10.1038/s41598-021-01246-x.

[6] S. Zhang, D. A. Genov, Y. Wang, M. Liu, and X. Zhang, “Plasmon-Induced Transparency in Metamaterials,” *Phys Rev Lett*, vol. 101, no. 4, p. 047401, Jul. 2008, doi: 10.1103/PhysRevLett.101.047401.

[7] F. Xue, S. Liu, and X. Kong, “Dual-band plasmon induced transparency metamaterial based on multi-quasi-bright modes,” *Phys Lett A*, vol. 413, p. 127556, Oct. 2021, doi: 10.1016/j.physleta.2021.127556.

[8] J. Han, J. Gu, Z. Tian, and W. Zhang, “Plasmon-induced transparency in terahertz metamaterials,” in *2012 37th International Conference on Infrared, Millimeter, and Terahertz Waves*, IEEE, Sep. 2012, pp. 1–2. doi: 10.1109/IRMMW-THz.2012.6380219.

[9] J.-T. Liu and Z. Liu, “Robust tunable plasmon induced transparency in coupled-resonance finite array of metasurface nanostructure,” *Sci Rep*, vol. 11, no. 1, p. 1221, Jan. 2021, doi: 10.1038/s41598-020-78795-0.

[10] M. Qin, L. Wang, X. Zhai, Q. Lin, and S. Xia, “Multispectral Plasmon Induced Transparency in a Defective Metasurface Plasmonic Nanostructure,” *IEEE Photonics Technology Letters*, vol. 30, no. 11, pp. 1009–1012, Jun. 2018, doi: 10.1109/LPT.2018.2829497.

[11] M. Jablan, H. Buljan, and M. Soljačić, “Plasmonics in graphene at infrared frequencies,” *Phys Rev B*, vol. 80, no. 24, p. 245435, Dec. 2009, doi: 10.1103/PhysRevB.80.245435.

[12] T. Stauber, N. M. R. Peres, and A. K. Geim, “Optical conductivity of graphene in the visible region of the spectrum,” *Phys Rev B*, vol. 78, no. 8, p. 085432, Aug. 2008, doi: 10.1103/PhysRevB.78.085432.

[13] W. Cui, Y. Wang, J. Xue, Z. He, and H. He, “Terahertz sensing based on tunable fano resonance in graphene metamaterial,” *Results Phys*, vol. 31, p. 104994, Dec. 2021, doi: 10.1016/j.rinp.2021.104994.

[14] H. Xu *et al.*, “Sensing analysis based on tunable Fano resonance in terahertz graphene-layered metamaterials,” *J Appl Phys*, vol. 123, no. 20, May 2018, doi: 10.1063/1.5029546.

[15] H.-T. Chen, W. J. Padilla, J. M. O. Zide, A. C. Gossard, A. J. Taylor, and R. D. Averitt, “Active terahertz metamaterial devices,” *Nature*, vol. 444, no. 7119, pp. 597–600, Nov. 2006, doi: 10.1038/nature05343.

[16] T. Dasri and A. Chingsungnoen, “Surface plasmon resonance enhanced light absorption and wavelength tuneable in gold-coated iron oxide spherical nanoparticle,” *J Magn Magn Mater*, vol. 456, pp. 368–371, Jun. 2018, doi: 10.1016/j.jmmm.2018.02.066.

[17] K. M. Devi, A. K. Sarma, D. R. Chowdhury, and G. Kumar, “Plasmon induced transparency effect through alternately coupled resonators in terahertz metamaterial,” *Opt Express*, vol. 25, no. 9, p. 10484, May 2017, doi: 10.1364/OE.25.010484.

[18] B. Zhang *et al.*, “Absorption and slow-light analysis based on tunable plasmon-induced transparency in patterned graphene metamaterial,” *Opt Express*, vol. 27, no. 3, p. 3598, Feb. 2019, doi: 10.1364/OE.27.003598.

[19] J. Ge *et al.*, “Tunable dual plasmon-induced transparency based on a monolayer graphene metamaterial and its terahertz sensing performance,” *Opt Express*, vol. 28, no. 21, p. 31781, Oct. 2020, doi: 10.1364/OE.405348.

[20] K. Matsunaga, Y. Hirai, Y. Neo, T. Matsumoto, and M. Tomita, “Tailored plasmon-induced transparency in attenuated total reflection response in a metal–insulator–metal structure,” *Sci Rep*, vol. 7, no. 1, p. 17824, Dec. 2017, doi: 10.1038/s41598-017-17847-4.

[21] D. Wu, J. Tian, L. Li, and R. Yang, “Plasmon induced transparency and refractive index sensing in a new type of graphene-based plasmonic waveguide,” *Opt Commun*, vol. 412, pp. 41–48, Apr. 2018, doi: 10.1016/j.optcom.2017.11.072.

[22] S. Xiao, T. Wang, T. Liu, X. Yan, Z. Li, and C. Xu, “Active modulation of electromagnetically induced transparency analogue in terahertz hybrid metal-graphene metamaterials,” *Carbon N Y*, vol. 126, pp. 271–278, Jan. 2018, doi: 10.1016/j.carbon.2017.10.035.

[23] Z. Vafapour and H. Alaei, “Subwavelength Micro-Antenna for Achieving Slow Light at Microwave Wavelengths via Electromagnetically Induced Transparency in 2D Metamaterials,” *Plasmonics*, vol. 12, no. 5, pp. 1343–1352, Oct. 2017, doi: 10.1007/s11468-016-0392-1.

[24] L. Ju *et al.*, “Graphene plasmonics for tunable terahertz metamaterials,” *Nat Nanotechnol*, vol. 6, no. 10, pp. 630–634, Oct. 2011, doi: 10.1038/nnano.2011.146.

[25] E. Gao *et al.*, “Dual dynamically tunable plasmon-induced transparency in H-type-graphene-based slow-light metamaterial,” *Journal of the Optical Society of America A*, vol. 36, no. 8, p. 1306, Aug. 2019, doi: 10.1364/JOSAA.36.001306.

[26] A. Yariv, “Coupled-mode theory for guided-wave optics,” *IEEE J Quantum Electron*, vol. 9, no. 9, pp. 919–933, Sep. 1973, doi: 10.1109/JQE.1973.1077767.

[27] *Handbook of Optical Constants of Solids*. Elsevier, 1985. doi: 10.1016/C2009-0-20920-2.

[28] C. H. Gan, H. S. Chu, and E. P. Li, “Synthesis of highly confined surface plasmon modes with doped graphene sheets in the midinfrared and terahertz frequencies,” *Phys Rev B*, vol. 85, no. 12, p. 125431, Mar. 2012, doi: 10.1103/PhysRevB.85.125431.

[29] M. Zhao *et al.*, “Tunable slow light effect based on dual plasmon induced transparency in terahertz planar patterned graphene structure,” *Results Phys*, vol. 15, p. 102796, Dec. 2019, doi: 10.1016/j.rinp.2019.102796.

[30] H. Cheng, S. Chen, P. Yu, X. Duan, B. Xie, and J. Tian, “Dynamically tunable plasmonically induced transparency in periodically patterned graphene nanostrips,” *Appl Phys Lett*, vol. 103, no. 20, p. 203112, Nov. 2013, doi: 10.1063/1.4831776.

[31] H. A. Haus and W. Huang, “Coupled-mode theory,” *Proceedings of the IEEE*, vol. 79, no. 10, pp. 1505–1518, 1991, doi: 10.1109/5.104225.

[32] K. L. Tsakmakidis *et al.*, “Breaking Lorentz reciprocity to overcome the time-bandwidth limit in physics and engineering,” *Science (1979)*, vol. 356, no. 6344, pp. 1260–1264, Jun. 2017, doi: 10.1126/science.aam6662.

[33] H. Xu *et al.*, “Sensing analysis based on tunable Fano resonance in terahertz graphene-layered metamaterials,” *J Appl Phys*, vol. 123, no. 20, May 2018, doi: 10.1063/1.5029546.

[34] T. Wei, F. Hauke, and A. Hirsch, “Evolution of Graphene Patterning: From Dimension Regulation to Molecular Engineering,” *Advanced Materials*, vol. 33, no. 45, Nov. 2021, doi: 10.1002/adma.202104060.